Communication

Low-Cost Nanocarbon-Based Peroxidases from Graphite and Carbon Fibers

Yan Zeng, Feifan Miao, Zhiyong Zhao, Yuting Zhu, Tao Liu, Rongsheng Chen, Simin Liu, Zaosheng Lv and Feng Liang * iD

The State Key Laboratory of Refractories and Metallurgy, School of Chemistry & Chemical Engineering, Wuhan University of Science and Technology, Wuhan 430081, China; zengyan@wust.edu.cn (Y.Z.); miaoff@cnnp.com.cn (F.M.); zhaozhiyong@wust.edu.cn (Z.Z.); zhuyt@nanoctr.cn (Y.Z.); liutaowust@163.com (T.L.); chenrs@wust.edu.cn (R.C.); liusimin@wust.edu.cn (S.L.); lvzaosheng@wust.edu.cn (Z.L.)

* Correspondence: feng_liang@whu.edu.cn; Tel.: +86-27-6886-2107

Abstract: A low-cost and facile preparation of water-soluble carbon nanomaterials from commercial available graphite and polypropylene carbon fibers was achieved. *N*-doped graphene quantum dot was also prepared as a comparable agent. The resultant carbon nanomaterials were characterized by vital techniques such as transmission electron microscopy (TEM), X-ray photoelectron spectroscopy (XPS), UV-vis absorption, Fourier transform infrared (FT-IR) and Raman spectra. The prepared carbon nanomaterials can make hydrogen peroxide degradation produce hydroxyl radicals, thus possess intrinsic peroxidase-like activity for colorimetric and UV-vis absorption detection of hydrogen peroxide. These carbon nanomaterials exhibit excellent sensitivity toward hydrogen peroxide with the limit of detection as low as 0.024 mM (by Carbon nanomaterials-1 from carbon fibers), 0.0042 mM (by Carbon nanomaterials-2 from graphite) and 0.014 mM (by Carbon nanomaterials-3 from nitrogen doped graphene oxide), respectively. The practical use of these carbon nanomaterials for phenolic compounds removal in aqueous solution is also demonstrated successfully. The extraordinary catalytic performance and low cost of these carbon nanomaterials make them a powerful tool for a wide range of potential applications.

Keywords: carbon nanomaterials; nanozyme; peroxidase mimetics; hydrogen peroxide; removal of phenolic compounds

1. Introduction

Artificial enzymes as highly stable and low-cost alternatives to natural enzymes hold a great potential and widespread application in biosensor and biomedicine [1]. Metal complexes, supramolecules and biomolecules have been extensively explored to mimic various intrinsic properties of natural enzymes [2]. Recently, nanoparticles (NPs) have attracted increasing attention because of their unique physicochemical properties, such as their comparable size to natural enzymes, high surface area to volume ratio, the presence of a large number of catalytically active sites on their surface and the availability of multifunctional reactive groups for modification and further functionalization [3,4]. In 2007, Gao et al. provided the first evidence that inert ferromagnetic nanoparticles have intrinsic peroxidase-like activity [5]. So far, it has been reported over 50 kinds of nanomaterials, which possess intrinsic activity similar to enzymes, such as magnetic nanoparticles, gold nanoparticles, platinum nanoparticles, cerium oxide nanoparticles and carbon nanomaterials [2–8].

Compared with nanomaterials of metals and their oxides, carbon nanomaterials have the advantages of diverse sources, low cost and less toxic in vivo [8–10]. It is also known that carbon nanomaterials can be used as nanotemplates for being functionalized with a wide range of

(bio)molecules, make it possible their application in different analytical areas or can be implemented in fields of nanomedicine, catalysis, electrocatalysis, electronics, optoelectronics and photovoltaics [11–15]. In 2010, Qu et al. reported the peroxidase-like activity of graphene oxide (GO) and its application to glucose detection [16]. Subsequently, Qu's and other several groups expanded GO to graphene nanocomposites [17], carbon nanotubes (CNTs) [18,19], carbon dots (CDs) [20–22] and graphene quantum dots (GQDs) [23–25] as peroxidase-like catalysts and further prepared GQD-band-aid for wound disinfection [26]. Recently, Chen et al. utilized dopamine as nitrogen source and GO as carbon source to prepare *N*-doped GQDs (*N*-GQDs) and found *N*-GQDs exhibited the enhanced peroxidase catalytic activity [27].

Although graphene quantum dots (GQDs) and doped GQDs have gained great attention owing to intrinsic peroxidase-like activity for colorimetric and UV-vis absorption detection, GQDs is typically prepared from expensive graphene oxide (GO, the price of 100 mg GO is about $15.6) with energy consumed microwave reaction of 12 h [26,27]. Very recently, we developed a one-pot solvothermal method to prepare carbon dots decorated graphite felt (CDs/GF) electrode, which exhibited excellent wettability and greatly enhanced activity towards vanadium redox couples [28,29]. Herein, we demonstrated the use of low-cost graphite (the price of 100 mg graphite is about $0.0056) and polypropylene carbon fibers (the price of 100 mg polypropylene carbon fibers is about $1.37) as carbon source for mixed acid preparation of carbon nanomaterials, and also prepared *N*-doped GQDs with cheap urea as nitrogen source and GO as carbon source. Three carbon nanomaterials were defined as Carbon nanomaterials-1 (prepared from carbon fibers), Carbon nanomaterials-2 (prepared from graphite), and Carbon nanomaterials-3 (prepared from nitrogen doped graphene oxide) in this manuscript. They were fully characterized by transmission electron microscope (TEM), X-ray photoelectron spectroscopy (XPS), Fourier transform infrared (FT-IR), Zeta potential measurements and Raman spectra. Subsequently, the peroxidase catalytic activities of these carbon nanomaterials were investigated and the catalytic mechanism was discussed. These carbon nanomaterials with peroxidase-like catalytic activity, taking Carbon nanomaterials-2 (prepared from graphite) as an example, were further applied to remove phenolic compounds, the pollutant in water.

2. Results and Discussion

2.1. Synthesis and Characterization of Carbon Nanomaterials

Three carbon nanomaterials, Carbon nanomaterials-1 (prepared from polypropylene carbon fibers), Carbon nanomaterials-2 (prepared from graphite), and Carbon nanomaterials-3 (nitrogen doped GQDs from GO) were prepared according to the the detail process in the Method section. All carbon nanomaterials were fully characterized by TEM (JEM-2010UHR microscopy, JEOL, Tokyo, Japan), XPS spectroscopy (ESCALAB250Xi, Thermo Fisher Scientific, Beijing, China), FT-IR (VERTEX 70, Bruker, Bremen, Germany), Zeta potential measurements (Zetasizer Nano-ZS ZEN3600 Malvern, Worcestershire, UK) and Raman spectra (INVIA plus Laser Raman Spectrometer, Renishaw, New Mills, UK).

First, the morphology and size of Carbon nanomaterials-1, Carbon nanomaterials-2 and Carbon nanomaterials-3 were characterized by TEM. The size distribution of Carbon nanomaterials-1, Carbon nanomaterials-2 and Carbon nanomaterials-3 is in the range of 2–5 nm, 3–8 nm and 1–3 nm respectively (Figure 1). X-ray photoelectron spectroscopy (XPS) was then used to characterize these carbon nanomaterials. As shown in Figure 2, the dominant graphitic C 1s peak at 284.8 eV and O 1s peak at 532 eV were observed for three carbon nanomaterials, and N 1s peak around 400 eV could be detected for Carbon nanomaterials-3. According to the deconvoluted XPS spectra of C 1s in Figure 3, there were C−C, C−O and −COOH on Carbon nanomaterials-1 surface, and C=O on Carbon nanomaterials-2 and Carbon nanomaterials-3 surface. The carbonyl group can act as substrate binding sites [30], which are beneficial to peroxidase like catalytic reaction. This can prove that the catalytic activity of Carbon nanomaterials-2 and Carbon nanomaterials-3 is better than that of Carbon nanomaterials-1.

The nitrogen element in Carbon nanomaterials-3 belongs to pyridine type nitrogen, and exists in the form of amino, amide or others (Figure 3). Therefore, all carbon nanomaterials with many hydrophilic functional groups, showed good solubility (up to 1 mg·mL^{-1}) in water, and the solution could keep stable for several months at room temperature.
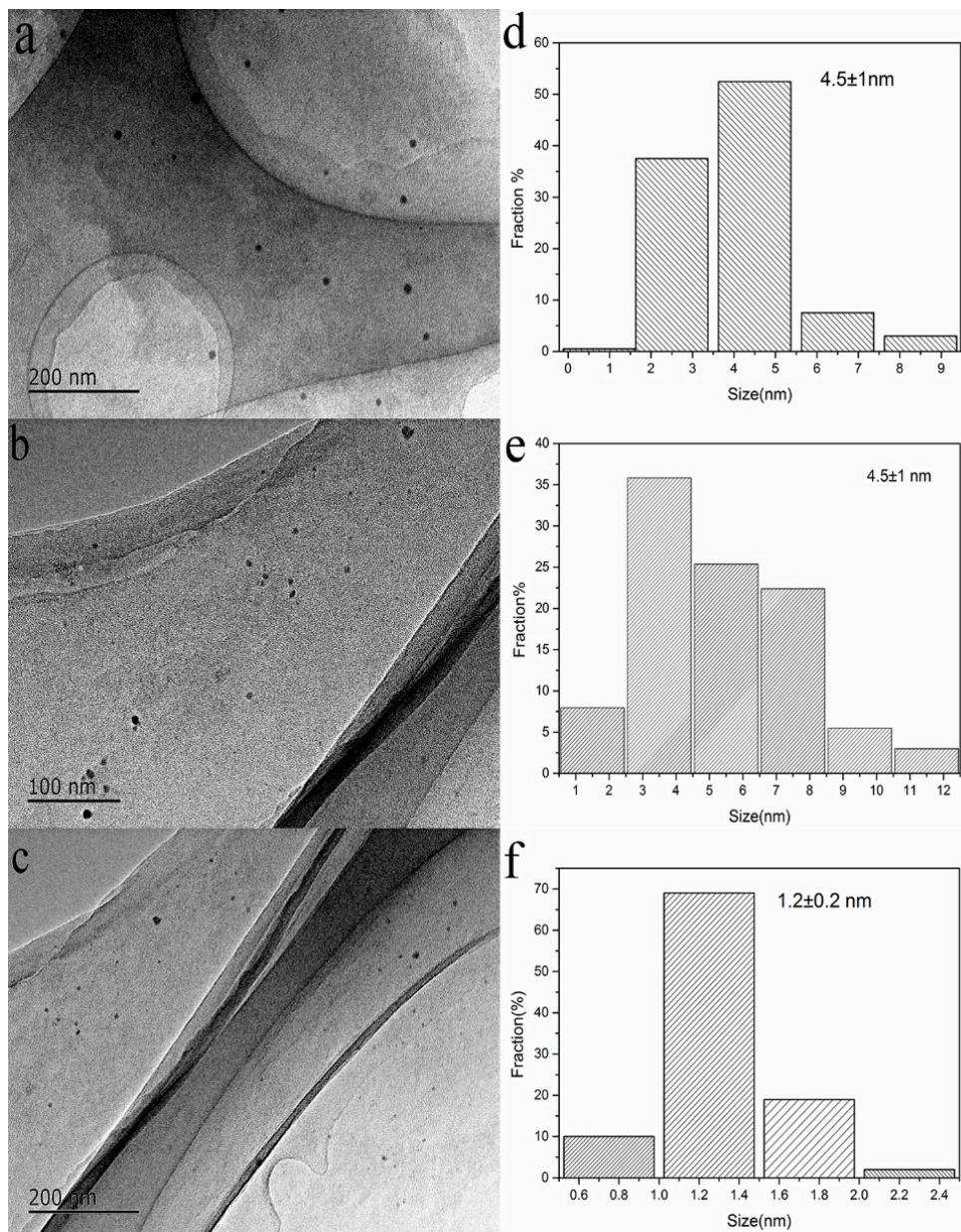

Figure 1. Typical transmission electron microscopy (TEM) images of synthesized carbon nanomaterials in this work: (**a**) Carbon nanomaterials-1; (**b**) Carbon nanomaterials-2; (**c**) Carbon nanomaterials-3; and diameter distribution of carbon nanomaterials; (**d**) Carbon nanomaterials-1; (**e**) Carbon nanomaterials-2; (**f**) Carbon nanomaterials-3.
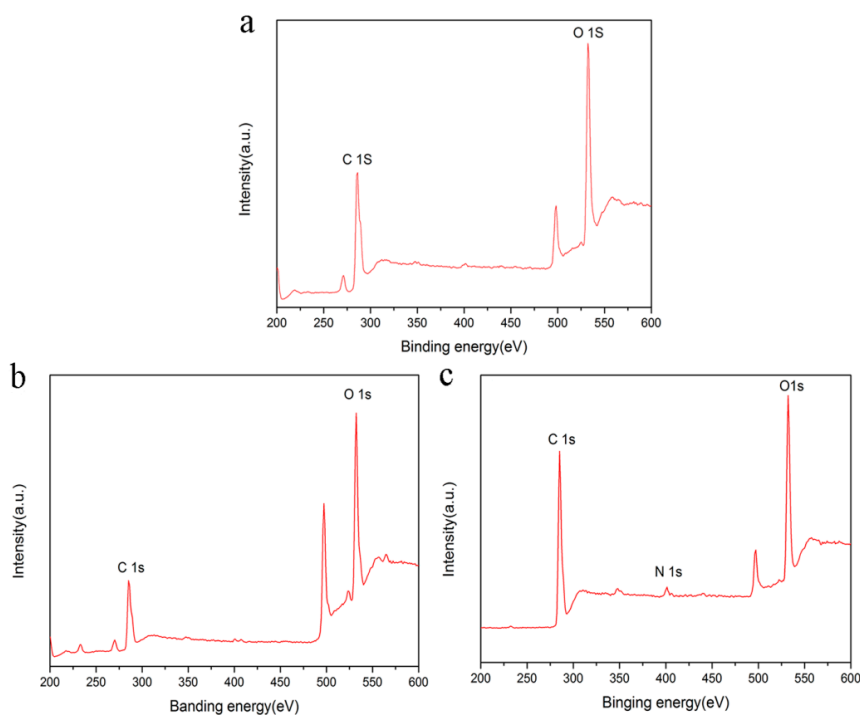
Figure 2. X-ray photoelectron spectroscopy (XPS) survey spectra of the as-synthesized carbon nanomaterials in this work: (**a**) Carbon nanomaterials-1; (**b**) Carbon nanomaterials-2; (**c**) Carbon nanomaterials-3.
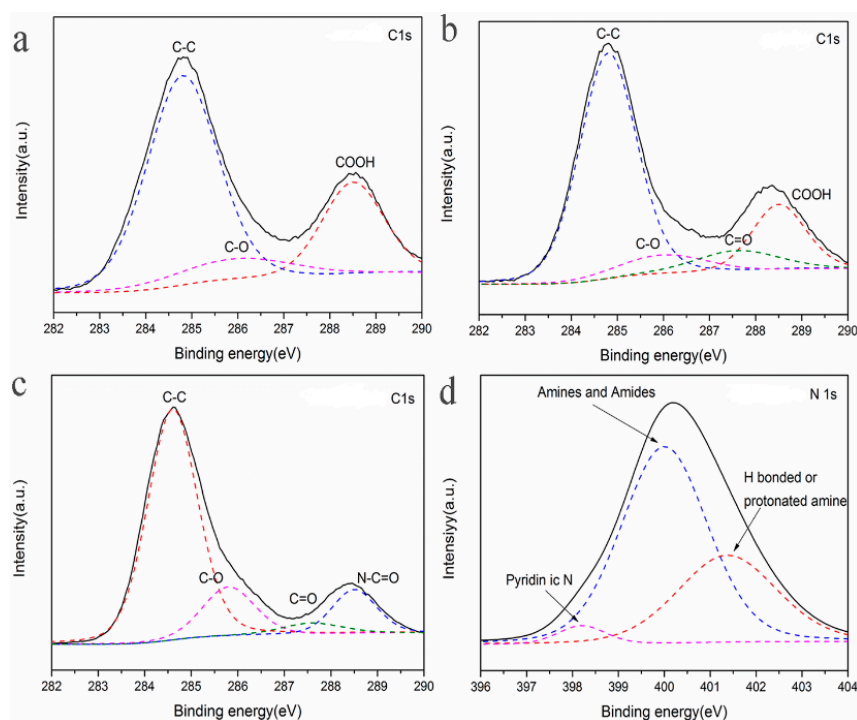

Figure 3. High-resolution XPS spectra of as-synthesized carbon nanomaterials in this work: (**a**) Carbon nanomaterials-1; (**b**) Carbon nanomaterials-2; (**c**,**d**) Carbon nanomaterials-3.

FT-IR spectroscopy (Figure S1) reveals the existence of O-H in different carbon nanomaterials, which can be seen from the obvious peak at 3650 cm^{-1}. The peak at 3000 cm^{-1} corresponds to the carboxyl group, and the peak at 1724 cm^{-1} in the spectrum of Carbon nanomaterials-2 is from the

carbonyl group. The Raman spectra illustrate the existence of 1350 cm^{-1} (D) and 1570 cm^{-1} (G) peaks in different carbon nanomaterials. The G peak means the sp^2 hybrid carbon atom and the D peak means the sp^3 hybrid carbon atom. The value of I_D/I_G represents the defect layer in the surface and the edge of the carbon material. To be specific, when the value of I_D/I_G is less than 1, some functional groups may be introduced into the carbon nanomaterials, thus endowing the nanomaterials with special properties (Figure S2). Among three kinds of carbon nanomaterials, Carbon nanomaterials-3 shows the highest I_D/I_G value owing to the introduction of nitrogen atoms. Besides, it is noticed that the value of the zeta potential changed a lot when doping nitrogen into the carbon (Figure S3).

2.2. The Peroxidase Catalytic Activities of Carbon Nanomaterials

It has been reported that some carbon nanomaterials have the peroxidase-like activity, which can catalyze the oxidation reaction between H_2O_2 and 3,3',5,5'-tetramethylbenzidine (TMB), resulting in a blue colored product [16]. In current system, after addition of both H_2O_2 and TMB into the Carbon nanomaterials-2 solution, the solution can change to blue (the tube 4 in Figure 4a). While only TMB solution or the TMB and H_2O_2 solution shows colorless (the tubes 1 and 2 in Figure 4a), and when adding TMB to the Carbon nanomaterials-2 solution, the solution shows brown due to the intrinsic color of Carbon nanomaterials-2 (the tube 3 in Figure 4a). Meanwhile, Carbon nanomaterials-1 and Carbon nanomaterials-3 have the same results in the color reaction. We noticed that there was no metal catalyst in these carbon nanomaterials from the XPS spectrum as shown in Figure 2. These result indicated that three carbon nanomaterials in our case possessed peroxidase-like catalytic activity. In addition, the profile of the time-dependent absorbance change at 652 nm (Figure 4b) indicated that the reaction rate and absorbance change greatly increased with increaseing of the Carbon nanomaterials-2 concentration. When the concentration of Carbon nanomaterials-2 is up to 40 μg·mL^{-1}, the reaction rate reaches the maximum value.

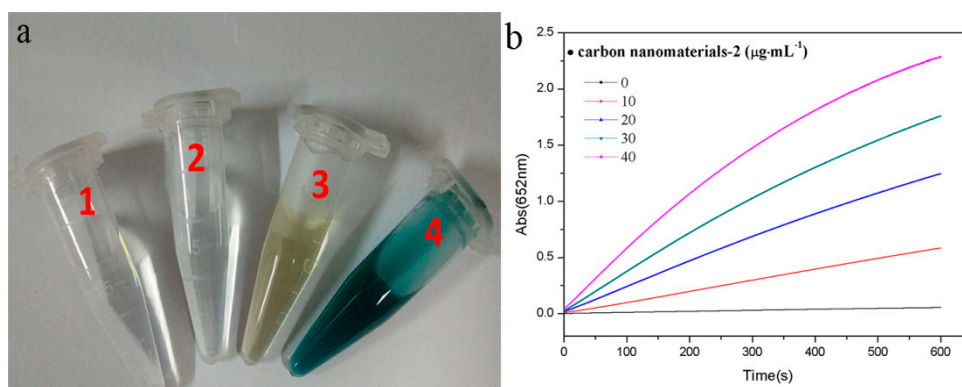**Figure 4.** (**a**) Typical photographs of 1 mL of 800 μM 3,3',5,5'-tetramethylbenzidine (TMB) reaction solutions oxidized by Carbon nanomaterials-2 in the presence of H_2O_2 after 5 min incubation at 35 °C in 25 mM phosphate buffer (pH 4.0): (1) 800 μM TMB; (2) 50 mM H_2O_2 and 800 μM TMB; (3) 800 μM TMB and 40 μg·mL^{-1} Carbon nanomaterials-2; (4) 50 mM H_2O_2, 800 μM TMB and 40 μg·mL^{-1} Carbon nanomaterials-2; (**b**) The time-dependent absorbance changes at 652 nm in the absence or presence of Carbon nanomaterials-2 in 25 mM phosphate buffer (pH 4.0) at 35 °C. The profile of the time-dependent absorbance were acquired with an UV-3600 UV-vis-NIR spectrometer (Shimadzu, Kyoto, Japan).

Typically, the catalytic activity of peroxidase-like carbon nanomaterials mainly depends on the pH value, temperature and concentration of H_2O_2. Figure S4a shows that the reaction is pH dependent, and the optimum pH value is 4.0, and the catalytic activity can be terminated by the addition of excess acid. As shown in Figure S4b, the temperature could consistantly accalerate the reaction in the tested range. Therefore the optimal temperature is kept at 35 °C, which is very beneficial for practical detection. Figure S4c shows the kinetic behaviors of H_2O_2 function system. In the presence of

fixed carbon nanomaterials, absorbance at 652 nm increases rapidly before 150 mM of H_2O_2 and then increases slightly after 150 mM of H_2O_2. The results demonstrate that the catalytic reaction is a H_2O_2 concentration-dependent process, and the system could be applied in the determination of H_2O_2.

The peroxidase catalytic activities of different carbon nanomaterials were compared in the oxidation reaction between H_2O_2 and TMB (Figure S5). The results show that the three kinds of carbon nanomaterials can significantly accelerate the reaction, of which Carbon nanomaterials-2 and Carbon nanomaterials-3 have better effects relative to Carbon nanomaterials-1. To further compare the catalytic activities of different carbon nanomaterials, state kinetic parameters were examined within an appropriate concentration range of TMB and H_2O_2. In the experiment, the concentration of one substrate is fixed, and the concentration of the other substrate is variable. The initial velocity of the reaction can be obtained by measuring the relationship curve of absorbance at 652 nm and time. Lineweaver-Burk plot is used to calculate Michaelis Menten constant (K_m) and maximum reaction rate (V_{max}) of the three kinds of carbon nanomaterials (Figure S6). Here, the K_m value reveals the binding affinity between enzymes and substrates, and the V_{max} value reveals the turnover number of enzymes, which reflects their catalytic activity [16].

As shown in Table 1, using TMB as the variable substrate, the K_m value of Carbon nanomaterials-1 is the highest, so that higher H_2O_2 concentration is necessary in order to get better catalytic activity. In contrast, the K_m values of Carbon nanomaterials-2 and Carbon nanomaterials-3 are very similar and relatively low, indicating that both of them have a good affinity with TMB. On the other hand, the V_{max} value of Carbon nanomaterials-2 is close to that of Carbon nanomaterials-3, but two times high as that of Carbon nanomaterials-1. Using H_2O_2 as the variable substrate, the K_m value of Carbon nanomaterials-3 is the lowest, which indicates that Carbon nanomaterials-3 have better affinity with H_2O_2 than others. However, Carbon nanomaterials-2 show the largest V_{max} value among the three kinds of carbon nanomaterials, which probably means more active sites on Carbon nanomaterials-2. It is noticed that the prepared carbon nanomaterials show lower K_m value and higher V_{max} value, and their V_{max} value is two orders of magnitude higher than that reported in previous literature [27]. Consequently, the three kinds of carbon nanomaterials have better catalytic activity than those reported in the previous literatures.

Table 1. Michaelis-Menten constant (K_m) and maximum reaction rate (V_{max}) of different carbon nanomaterials in this work and references.

Catalyst	Substrate Varied	Substrate Fixed (mM)	K_m (mM)	V_{max} (10^{-8} M·s^{-1})
Carbon nanomaterials-1 (this work)	TMB (3,3′,5,5′-Tetramethylbenzidine)	H_2O_2 (25)	2.45	155.9
Carbon nanomaterials-1 (this work)	H_2O_2	TMB (0.2)	0.01	10.31
Carbon nanomaterials-2 (this work)	TMB	H_2O_2 (5)	1.06	337.7
Carbon nanomaterials-2 (this work)	H_2O_2	TMB (0.2)	0.001	55.13
Carbon nanomaterials-3 (this work)	TMB	H_2O_2 (5)	0.97	328.5
Carbon nanomaterials-3 (this work)	H_2O_2	TMB (0.2)	0.0006	27.69
N-GQDs (*N*-doped graphene quantum dots) (Ref. [27])	TMB	H_2O_2 (3.3)	11.2	0.38
N-GQDs (Ref. [27])	H_2O_2	TMB (0.3)	0.10	0.14

2.3. H_2O_2 Detection Utilizing Carbon Nanomaterials

Our system could be applied in the determination of H_2O_2 because the peroxidase-like activity of carbon nanomaterials is dependent on the concentration of H_2O_2. As shown in Figure 5a,c,e, the absorbance keep increasing with the increase of H_2O_2 concentration and the color reaction is obvious, which may be observed by naked eyes. As can be seen in Figure 5b,d,f, the absorbance at 652 nm shows a good linear relationship with the concentration of H_2O_2 in the range of 0.02~0.2 mM when Carbon nanomaterials-1 and Carbon nanomaterials-2 are used. In the case of Carbon nanomaterials-1, the linear regression equation is $A = 0.34C + 0.043$ with a correlation coefficient

of 0.9937; in the case of Carbon nanomaterials-2, the linear regression equation is $A = 1.484C + 0.065$ with a correlation coefficient of 0.9943. In the case of Carbon nanomaterials-3, as the H_2O_2 concentration changes from 0.02 to 0.4 mM, the linear regression equation is $A = 0.637C + 0.032$ with a correlation coefficient of 0.9884. The detection limit of the method using Carbon nanomaterials-1, Carbon nanomaterials-2, Carbon nanomaterials-3 are 0.024 mM, 0.0042 mM and 0.014 mM, respectively. It has been reported that the presence of functional group could affect peroxidase-like activity of carbon nanomaterials [30]. The ketonic carbonyl groups act as the catalytically active sites and the carboxylic groups serve as the substrate-binding sites. The existence of phenol and alcohol groups decreases the catalytic activity of carbon nanomaterials. The Carbon nanomaterials-2 prepared from natural graphite has better catalytic activity than Carbon nanomaterials-1 prepared from carbon fibers. The possible reason is that the surface of the Carbon nanomaterials-2 contains more ketonic carbonyl groups and carboxylic groups than that of Carbon nanomaterials-1 (Figure 3).
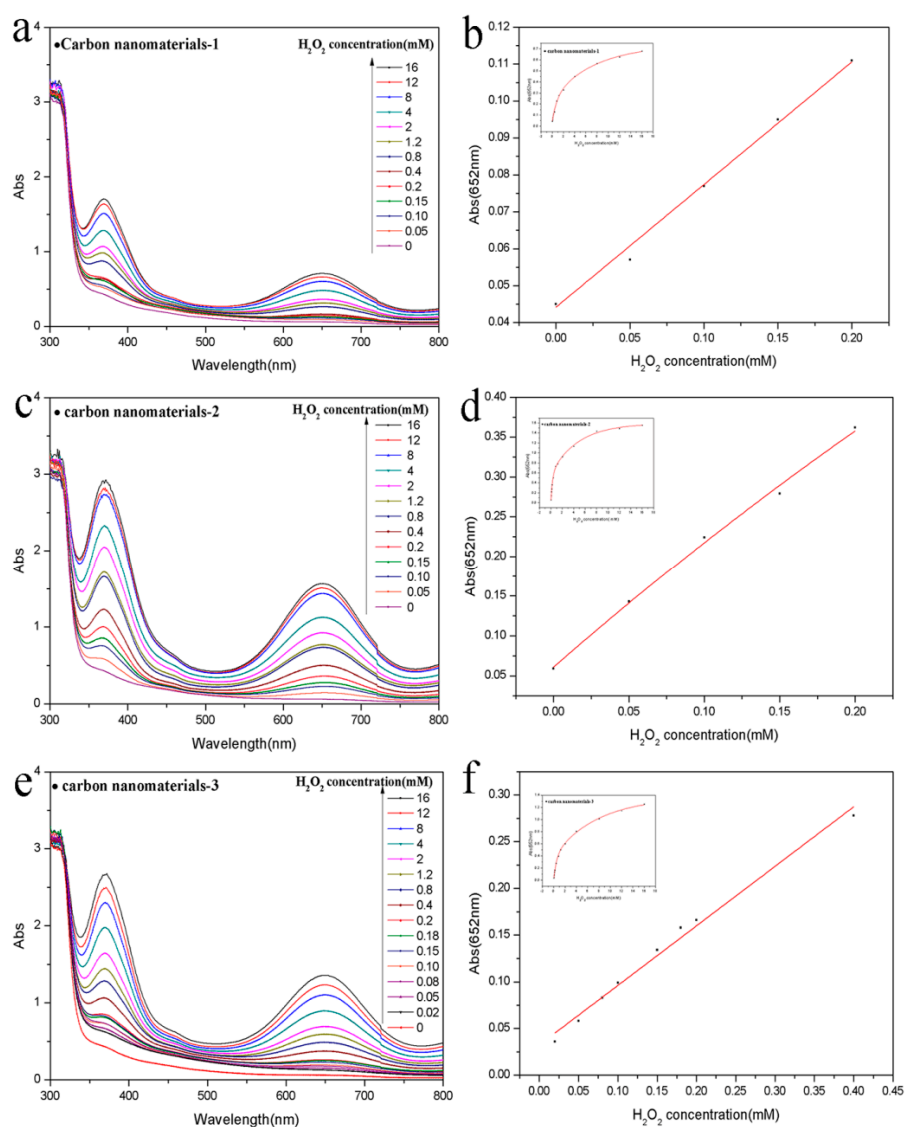

Figure 5. UV-vis absorption spectra and linear calibration plot for H_2O_2 detection using (**a**,**b**): Carbon nanomaterials-1; (**c**,**d**): Carbon nanomaterials-2; (**e**,**f**): Carbon nanomaterials-3. The solution of 800 μM TMB was treated with 40 μg·mL^{-1} carbon nanomaterials in phosphate buffer (pH 4.0) at 35 °C. The concentration of H_2O_2 was changed from 0 to 16 mM. The absorption spectra were acquired with an UV-3600 UV-vis-NIR spectrometer (Shimadzu, Kyoto, Japan).

2.4. Catalytic Mechanism of Carbon Nanomaterials

The peroxidase-like properties of carbon nanomaterials may originate from their catalytic ability, which can make hydrogen peroxide degradation produce hydroxyl radicals (•OH) [16]. In this study, fluorescence experiments are carried out to detect •OH during the reaction. •OH can be captured by terephthalic acid (TA) as a fluorescence probe and generate 2-hydroxyl terephthalic acid (TAOH), which can emit unique fluorescence at 435 nm (Figure 6a). As shown in Figure 6b–d, three kinds of carbon nanomaterials present the same variation trend in fluorescence intensity after 24 h, and the fluorescence intensity of the solution with TA, H_2O_2 and carbon nanomaterials is significantly enhanced. These results prove the presence of •OH during the interaction between carbon nanomaterials and H_2O_2. Similar to peroxidase mimics with iron centers, electron transfer may occur between pairs of different oxidation states of carbon nanomaterials, which can promote their catalytic activity.
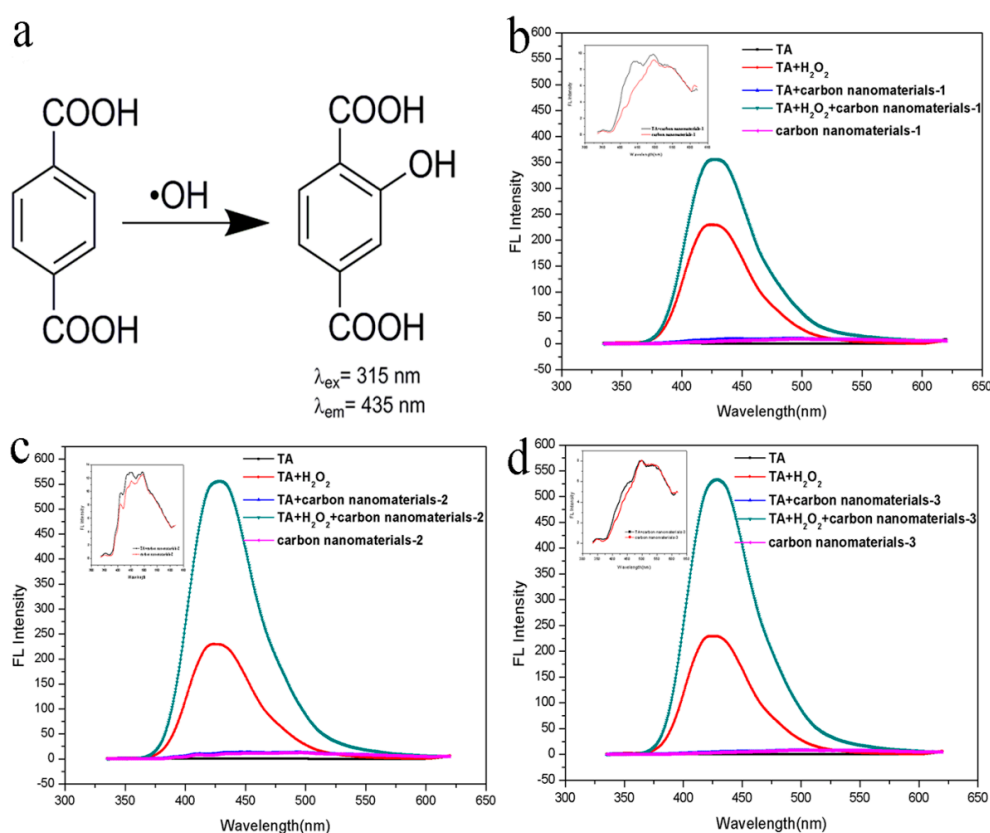

Figure 6. (**a**) Reaction between hydroxyl radica •OH and terephthalic acid (TA). Fluorescence spectra of TA with/without H_2O_2 treated 24 h with carbon nanomaterials; (**b**) Carbon nanomaterials-1; (**c**) Carbon nanomaterials-2; (**d**) Carbon nanomaterials-3. In the reaction system, the TA, H_2O_2 and carbon nanomaterials were 0.5 mM, 1 mM, and 20 µg·mL^{-1}, respectively. The fluorescence spectra were acquired with a LS55 fluorescence spectrometer (PerkinElmer, Waltham, MA, USA).

2.5. Phenolic Compounds Removal Utilizing Carbon Nanomaterials

The removal of phenolic compounds using different carbon nanomaterials as the catalyst in presence of H_2O_2 was explored. In a typical procedure [31], 1 mg of carbon nanomaterials was added into 1 mL of NaAc buffer (0.1 M, pH 3.5) containing 6 mM of phenol and 30 mM of H_2O_2, and then incubated at 30 °C for 24 h. After 24 h of reaction, the residual phenolic compounds present in the supernatant was measured with potassium ferricyanide and 4-aminoantipyrine, to determin the removal efficiency by measuring the absorbance of the phenol complex at 490 nm(Figure 7a). It was found that 12.03%, 55.7% and 71.7% of the phenol were removed by Carbon nanomaterials-1, Carbon

nanomaterials-2 and Carbon nanomaterials-3 (Figure 7b). Carbon nanomaterials-2 was further used to remove homologues of phenol under the same condition. Among tested phenolic compounds, the removal effiency of 2,4-dichlorophenol was 23.64%, the removal effiency of 4-methoxyphenol was 56.35%, the removal effiency of resorcinol was 21.2%.
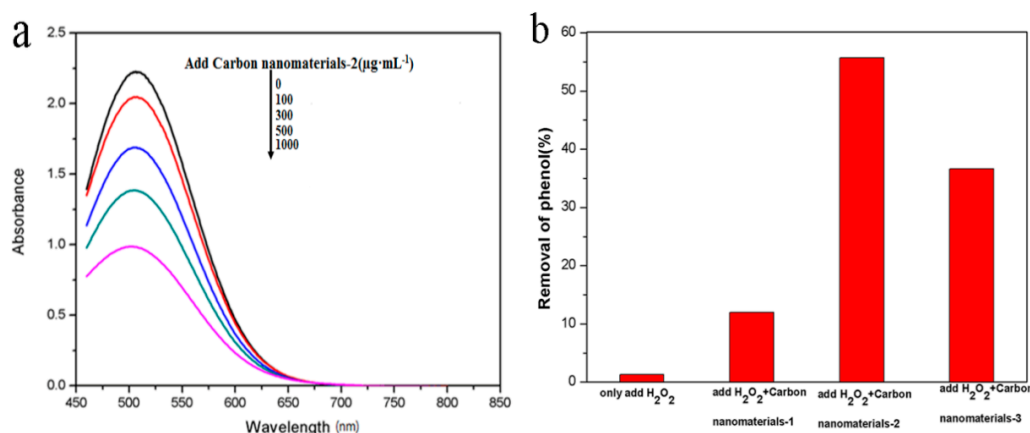

Figure 7. (**a**) UV-vis absorption spectra of the products obtained by chromogenic reaction of phenol. Different concentrations of Carbon nanomaterials-2 were added into 1 mL of NaAc buffer (0.1 M, pH 3.5) containing 6 mM of phenol and 30 mM of H_2O_2, and then incubated at 30 °C for 24 h. After the residual phenol in these solutions had chromogenic reaction, its absorption curve was determined by an UV-3600 UV-vis-NIR spectrometer (Shimadzu, Kyoto, Japan); (**b**) Removal efficiency (%) of phenol when added various carbon nanomaterials.

3. Materials and Methods

3.1. Synthesis of Carbon Nanomaterials-1 and Carbon Nanomaterials-2

The synthesis details of Carbon nanomaterials-2 were described as follows [23,32]. Commercially available graphite powder or milled carbon fiber powder (300 mg) was added into a mixture of concentrated H_2SO_4 (95%, 60 mL) and HNO_3 (65%, 20 mL). The suspension was sonicated for 2 h, then refluxed for additional 24 h. Afterwards, the mixture was cooled to room temperature and diluted with deionized water to 800 mL. Successively, the pH value of the reaction solution was adjusted to 8 with Na_2CO_3. After the suspension was concentrated to 50 mL and filtered to remove the precipitated inorganic salts. The filtrate was collected and further dialyzed in a dialysis bag (3000 molar mass cutoff) for 7 days. Carbon nanomaterials-2 or Carbon nanomaterials-1 powder could be obtained by freeze-drying.

3.2. Synthesis of Carbon Nanomaterials-3

Firstly, GO was prepared from graphite by following the method reported by Yan et al. [33] in a typical synthesis. 4 g of urea was added into 20 mL of GO aqueous suspension (1 mg·mL^{-1}), and the mixture was ultra-sonicated for 2 h. Then, 18 mL mixture was transferred to a Teflon-lined stainless steel autoclave with a volume of 20 mL. The mixture was sealed and heated at 170 °C for 12 h. The resultant Carbon nanomaterials-3 was filtered, washed and dispersed in water [34].

4. Conclusions

In summary, graphite, polypropylene carbon fibers and GO were used as raw materials to synthesize Carbon nanomaterials-2, Carbon nanomaterials-1 and Carbon nanomaterials-3. The peroxidase-like activities of resultant carbon nanomaterials were determined. It was found that carbon nanomaterials had similar properties to natural enzymes, which closely depended on the pH value, temperature, and the concentration of H_2O_2. According to kinetic analysis, Carbon nanomaterials-3 had the best catalytic

activity, Carbon nanomaterials-2 showed similar catalytic activity to Carbon nanomaterials-3 and catalytic activity of Carbon nanomaterials-1 was the lowest. Considering the synthetic process and the cost of raw materials, Carbon nanomaterials-2 synthesized from graphite could function as one kind of ideal substitute for natural enzymes. In addition, these carbon nanomaterials could be used to quantitatively determine the concentration of H_2O_2 by using a simple, rapid, highly selective and sensitive colorimetric method. It was also demonstrated that as-obtained three carbon nanomaterials exhibited comparable catalytic efficiency for some phenolic compounds removal.

Supplementary Materials: The following are available online at http://www.mdpi.com/2076-3417/7/9/924/s1, Figure S1: FT-IR Spectrometer of as-synthesized carbon nanomaterials in this work; Figure S2: Raman spectra of as-synthesized carbon nanomaterials in this work; Figure S3: Zeta potential of as-synthesized carbon nanomaterials in this work; Figure S4: Effects of pH value, temperature and H_2O_2 concentrations on the peroxidase catalytic activities of different carbon nanomaterials; Figure S5: The time-dependent absorbance at 652 nm in the presence of 40 $\mu g \cdot mL^{-1}$ different carbon nanomaterials; Figure S6: The kinetic behaviors for as-prepared carbon nanomaterials.

Author Contributions: Y.Z. and F.L. conceived and designed the experiments; Y.Z., F.M., Y.Z. and T.L. performed the experiments; Y.Z. and F.L. analyzed the data; R.C., S.L. Z.L. contributed reagents/materials/analysis tools; Y.Z., Z.Z. and F.L. wrote the paper.

Conflicts of Interest: The authors declare no conflict of interest.

References

1. Breslow, R.; Overman, L.E. Artificial enzyme combing a metal catalytic group and a hydrophobic binding cavity. *J. Am. Chem. Soc.* **1970**, *92*, 1075–1077. [CrossRef] [PubMed]

2. Wei, H.; Wang, E. Nanomaterials with enzyme-like characteristics (nanozymes): Next-generation artificial enzymes. *Chem. Soc. Rev.* **2013**, *42*, 6060–6093. [CrossRef] [PubMed]

3. Kuah, E.; Toh, S.; Yee, J.; Ma, Q.; Gao, Z. Enzyme mimics: Advances and applications. *Chem. Eur. J.* **2016**, *22*, 8404–8430. [CrossRef] [PubMed]

4. Wang, X.; Hu, Y.; Wei, H. Nanozymes in bionanotechnology: From sensing to therapeutics and beyond. *Inorg. Chem. Front.* **2016**, *3*, 41–60. [CrossRef]

5. Gao, L.; Zhuang, J.; Nie, L.; Zhang, J.; Zhang, Y.; Gu, N.; Wang, T.; Feng, J.; Yang, D.; Perrett, S.; et al. Intrinsic peroxidase-like activity of ferromagnetic nanoparticles. *Nat. Nanotechnol.* **2007**, *2*, 577–583. [CrossRef] [PubMed]

6. Lin, Y.; Ren, J.; Qu, X. Catalytically active nanomaterials: A promising candidate for artificial enzymes. *Acc. Chem. Res.* **2014**, *47*, 1097–1105. [CrossRef] [PubMed]

7. Gao, L.; Yan, X. Nanozymes: An emerging field bridging nanotechnology and biology. *Sci. China Life Sci.* **2016**, *59*, 400–402. [CrossRef] [PubMed]

8. Garg, B.; Bisht, T. Carbon nanodots as peroxidase nanozymes for biosensing. *Molecules* **2016**, *21*, 1653–1668. [CrossRef] [PubMed]

9. Zhou, X.; Liang, F. Application of graphene/graphene oxide in biomedicine and biotechnology. *Curr. Med. Chem.* **2014**, *21*, 855–869. [CrossRef] [PubMed]

10. Sun, H.; Ren, J.; Qu, X. Carbon nanomaterials and DNA: From molecular recognition to applications. *Acc. Chem. Res.* **2016**, *49*, 461–470. [CrossRef] [PubMed]

11. Jariwala, D.; Sangwan, V.K.; Lauhon, L.J.; Marks, T.J.; Hersam, M.C. Carbon nanomaterials for electronics, optoelectronics, photovoltaics, and sensing. *Chem. Soc. Rev.* **2013**, *42*, 2824–2860. [CrossRef] [PubMed]

12. Maas, M. Carbon nanomaterials as antibacterial colloids. *Materials* **2016**, *9*, 617–635. [CrossRef] [PubMed]

13. Muňoz, J.; Baeza, M. Customized bio-functionalization of nanocomposite carbon paste electrodes for electrochemical sensing: A mini review. *Electroanalysis* **2017**, *29*, 1660–1669. [CrossRef]

14. Liu, H.; Zhang, L.; Yan, M.; Yu, J. Carbon nanostructures in biology and medicine. *J. Mater. Chem. B* **2017**, *5*, 6437–6450. [CrossRef]

15. Navalon, S.; Herance, J.R.; Alvaro, M.; García, H. Covalently modified graphenes in catalysis, electrocatalysis and photoresponsive materials. *Chem. Eur. J.* **2017**. [CrossRef] [PubMed]

16. Song, Y.; Qu, K.; Zhao, C.; Ren, J.; Qu, X. Graphene oxide: Intrinsic peroxidase catalytic activity and its application to glucose detection. *Adv. Mater.* **2010**, *22*, 2206–2210. [CrossRef] [PubMed]

17. Singh, S.; Mitra, K.; Shukla, A.; Singh, R.; Gundampati, R.K.; Misra, N.; Maiti, P.; Ray, B. Brominated graphene as mimetic peroxidase for sulfide ion recognition. *Anal. Chem.* **2017**, *89*, 783–791. [CrossRef] [PubMed]

18. Song, Y.; Qu, K.; Xu, C.; Ren, J.; Qu, X. Visual and quantitative detection of copper ions using magnetic silica nanoparticles clicked on multiwalled carbon nanotubes. *Chem. Commun.* **2010**, *46*, 6572–6574. [CrossRef] [PubMed]

19. Song, Y.; Wang, X.; Zhao, C.; Qu, K.; Ren, J.; Qu, X. Label-free colorimetric detection of single nucleotide polymorphism by using single-walled carbon nanotube intrinsic peroxidase-like activity. *Chem. Eur. J.* **2010**, *16*, 3617–3621. [CrossRef] [PubMed]

20. Shan, X.; Chai, L.; Ma, J.; Qian, Z.; Chen, J.; Feng, H. B-doped carbon quantum dots as a sensitive fluorescence probe for hydrogen peroxide and glucose detection. *Analyst* **2014**, *139*, 2322–2325. [CrossRef] [PubMed]

21. Shi, W.; Wang, Q.; Long, Y.; Cheng, Z.; Chen, S.; Zheng, H.; Huang, Y. Carbon nanodots as peroxidase mimetics and their applications to glucose detection. *Chem. Commun.* **2011**, *47*, 6695–6697. [CrossRef] [PubMed]

22. Wu, D.; Deng, X.; Huang, X.; Wang, K.; Liu, Q. Low-cost preparation of photoluminescent carbon nanodots and application as peroxidase mimetics in colorimetric detection of H_2O_2 and glucose. *J. Nanosci. Nanotechnol.* **2013**, *13*, 6611–6616. [CrossRef] [PubMed]

23. Luo, P.; Ji, Z.; Li, C.; Shi, G. Aryl-modified graphene quantum dots with enhanced photoluminescence and improved pH tolerance. *Nanoscale* **2013**, *5*, 7361–7367. [CrossRef] [PubMed]

24. Zheng, X.T.; Ananthanarayanan, A.; Luo, K.Q.; Chen, P. Glowing graphene quantum dots and carbon dots: Properties, syntheses, and biological applications. *Small* **2015**, *11*, 1620–1636. [CrossRef] [PubMed]

25. Wu, Z.L.; Liu, Z.X.; Yuan, Y.H. Carbon dots: Materials, synthesis, properties and approaches to long-wavelength and multicolor emission. *J. Mater. Chem. B* **2017**, *5*, 3794–3809. [CrossRef]

26. Sun, H.; Gao, N.; Dong, K.; Ren, J.; Qu, X. Graphene quantum dots-band-aids used for wound disinfection. *ACS Nano* **2014**, *8*, 6202–6210. [CrossRef] [PubMed]

27. Lin, L.; Song, X.; Chen, Y.; Rong, M.; Zhao, T.; Wang, Y.; Jiang, Y.; Chen, X. Intrinsic peroxidase-like catalytic activity of nitrogen-doped graphene quantum dots and their application in the colorimetric detection of H_2O_2 and glucose. *Anal. Chim. Acta* **2015**, *869*, 89–95. [CrossRef] [PubMed]

28. Zhou, Y.; Liu, L.; Shen, Y.; Wu, L.; Yu, L.; Liang, F.; Xi, J. Carbon dots promoted vanadium flow batteries for all-climate energy storage. *Chem. Commun.* **2017**, *53*, 7565–7568. [CrossRef] [PubMed]

29. Zhou, Y.; Yu, L.; Wang, J.; Liu, L.; Liang, F.; Xi, J. Rational use and reuse of Nafion 212 membrane in vanadium flow batteries. *RSC Adv.* **2017**, *7*, 19425–19433. [CrossRef]

30. Sun, H.; Zhao, A.; Gao, N.; Li, K.; Ren, J.; Qu, X. Deciphering a nanocarbon-based artificial peroxidase: Chemical identification of the catalytically active and substrate-binding sites on graphene quantum dots. *Angew. Chem. Int. Ed.* **2015**, *54*, 7176–7180. [CrossRef] [PubMed]

31. Wu, X.; Zhang, Y.; Han, T.; Wu, H.; Guo, S.; Zhang, J. Composite of graphene quantum dots and Fe_3O_4 nanoparticles: Peroxidase activity and application in phenolic compound removal. *RSC Adv.* **2014**, *4*, 3299–3305. [CrossRef]

32. Peng, J.; Gao, W.; Gupta, B.K.; Liu, Z.; Romero-Aburto, R.; Ge, L.; Song, L.; Alemany, L.B.; Zhan, X.; Gao, G.; et al. Graphene quantum dots derived from carbon fibers. *Nano Lett.* **2012**, *12*, 844–849. [CrossRef] [PubMed]

33. Yan, X.; Chen, J.; Yang, J.; Xue, Q.; Miele, P. Fabrication of free-standing, electrochemically active, and biocompatible graphene oxide-polyaniline and graphene-polyaniline hybrid papers. *ACS Appl. Mater. Interfaces* **2010**, *2*, 2521–2529. [CrossRef] [PubMed]

34. Wu, J.; Zhang, D.; Wang, Y.; Hou, B. Electrocatalytic activity of nitrogen-doped graphene synthesized via a one-pot hydrothermal process towards oxygen reduction reaction. *J. Power Sources* **2013**, *227*, 185–190. [CrossRef]